Plasma kinetics around a dust grain in an ion flow

S. A. Maiorov,* S. V. Vladimirov,† and N. F. Cramer
Department of Theoretical Physics, School of Physics, The University of Sydney, New South Wales 2006, Australia
(Received 19 July 2000; published 19 December 2000)

The kinetics of plasma particles around a stationary dust grain in the presence of an ion flow is studied using a three-dimensional molecular dynamics simulation method. The model is self-consistent, involving the dynamics of plasma electrons and ions as well as charging of the dust grain. The effect of ion focusing is investigated as a function of the ion flow velocity. Distributions of electron and ion number densities, and electrostatic plasma potential are obtained.

DOI: 10.1103/PhysRevE.63.017401 PACS number(s): 52.27.Lw, 52.25.Vy, 52.35.Fp, 52.40.Hf

The dust structures in a low-temperature weakly ionized plasma have attracted considerable recent attention associated with colloidal crystals [1–4] as well as with other self-organized formations such as dust clouds, ''drops,'' ''voids,'' etc. [5–9]. In a typical laboratory discharge, dust particles are negatively charged and usually levitate in the sheath or presheath region under the balance of gravitational, electrostatic (due to the sheath electric field) and plasma (such as the ion drag) forces. The ion flow provides not only a direct (dragging) influence (supporting, e.g., the formation of dust voids [6,7]), but is also responsible for the generation of associated collective plasma processes which can strongly affect the vertical arrangement of dust grains [10–16]. The complete problem of plasma dynamics around a macroscopic body in the presence of plasma flows is highly nonlinear and therefore its numerical analysis is of major importance. Among various numerical methods, direct integration of the equations of motions of plasma particles represents a numerical experiment whose significance approaches experiments in the laboratory.

Previously, various models of dust in the presence of plasma flows were numerically considered, see, e.g., Refs. [11,13,17–20]. Note that the previous models deal with the fluid description of a plasma [11], the kinetic (i.e., coupled Poisson-Vlasov equations) case [19] without collisions in the vicinity of a dust grain, as well as with particle-in-cell simulations [18] of a uniform, steady state dc plasma where plasma particle losses are assumed to be exactly balanced by a constant ionization source, or a hybrid model [17] combining Monte Carlo with fluid simulation, with the latter ignoring the equations of motion of the plasma particles. In a non-self-consistent three-dimensional description [13], the ion-ion interactions were neglected and the charge of a dust particle was fixed. In the latest simulation [20], the structure of the wake potential behind a stationary pointlike dust grain with a constant charge was studied on ion time scales using particle-in-cell simulation methods; the ion dynamics (on a background of Boltzmann distributed electrons) was studied in one and two dimensions.

Here, we present the results of a self-consistent molecular dynamics (MD) three-dimensional (3D) simulation of the kinetics of plasma particles (electrons and ions) around a dust grain, taking into account the dust charging. The technique of studying the properties of a classical Coulomb plasma involving numerical integration of the equations of multiparticle dynamics used in this work is described in Refs. [21,22]. The core of the method includes consideration of the time evolution of the system consisting of N_i positively (''ions'' with $Z_i=1$) and N_e negatively (''electrons'') charged particles confined in a region $0<x<L_x$, $0<y<L_y$, $0<z<L_z$, together with a macroscopic absorbing grain (''dust particle'') of radius R with infinite mass and an initial (negative) charge $Q=-Z_d e$, where $-e$ is the electron charge. The dust grain is placed at $x=x_0$, $y=y_0$, and $z=z_0$. The walls bounding the simulation region are elastic for electrons; for ions, they are elastic in the y and z directions, i.e., at $y=(0,L_y)$ and $z=(0,L_z)$. The ions are introduced in the system at the plane $x=0$ as a uniform flow with the Mach number $M=V_0/c_s$ $(V_0>0)$ and the temperature T_i, where $c_s=(5T_e/3m_i)^{1/2}$ is the sound speed, T_e is the temperature of electrons (all temperatures are in energy units, i.e., Boltzmann's constant is unity), and m_i is the ion mass; at $x=L_x$ the ions are removed from the system. The paths of the ions and electrons are determined through numerical integration of the equations of motion $d^2\mathbf{r}_k/dt^2=\mathbf{F}_k/m_k$, where $\mathbf{F}_k=\Sigma_1^{1+N_i+N_e}\mathbf{f}_{kl}$ and the Coulomb force is given by $\mathbf{f}_{kl}=q_k q_l \mathbf{r}_{kl}/|\mathbf{r}_{kl}|^3$. For the characteristic lengths we have (for most calculations unless otherwise specified) $L_x/4=L_y=L_z=10\times h_x$, with the characteristic grid step in the presented results $h_x=4h_y=4h_z=1.077\,\mu$m. Other initial values are summarized in Table I. For the given values, the characteristic lengths in the plasma are: electron Debye

TABLE I. The initial values for the dust grain plasma particles. $m_p=1842m_e$ is the proton mass, $m_e=9.11\times10^{28}$ g is the electron mass, $e=4.8\times10^{-10}$ statCoul is the (absolute) electron charge.

	Macroparticle	Ions	Electrons
Charge	$-1000e$	e	$-e$
Mass	∞	$4m_p$	$100m_e$
Number	1	10 000	9000
Temperature	*n/a*	0.025 eV	1 eV

*Permanent address: Department of Theoretical Physics, General Physics Institute, Moscow 117942, Russia.

†Electronic address: S. Vladimirov@physics.usyd.edu.au; URL http://www.physics.usyd.edu.au/~vladimi

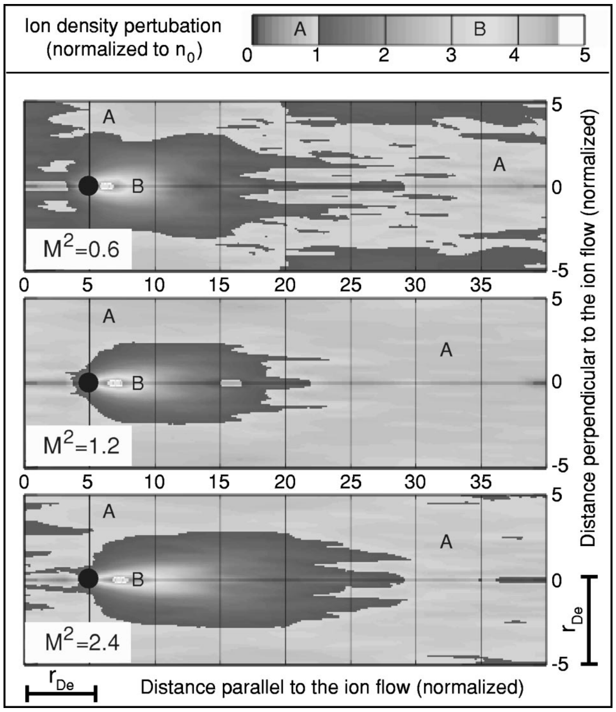

FIG. 1. Contour plot of the ion density, showing ion focusing, for three different velocities of ion flow. The plot is presented in the grayscale topograph style; regions A correspond to ion densities below 1, and regions B correspond to ion densities above 1. The ions are focusing behind the grain thus forming the region with highly enhanced ion density. The distances are given in the units of $h_x \approx 1.077\ \mu$m used in the calculation; the physical distance corresponding to the electron Debye length r_{De} is presented.

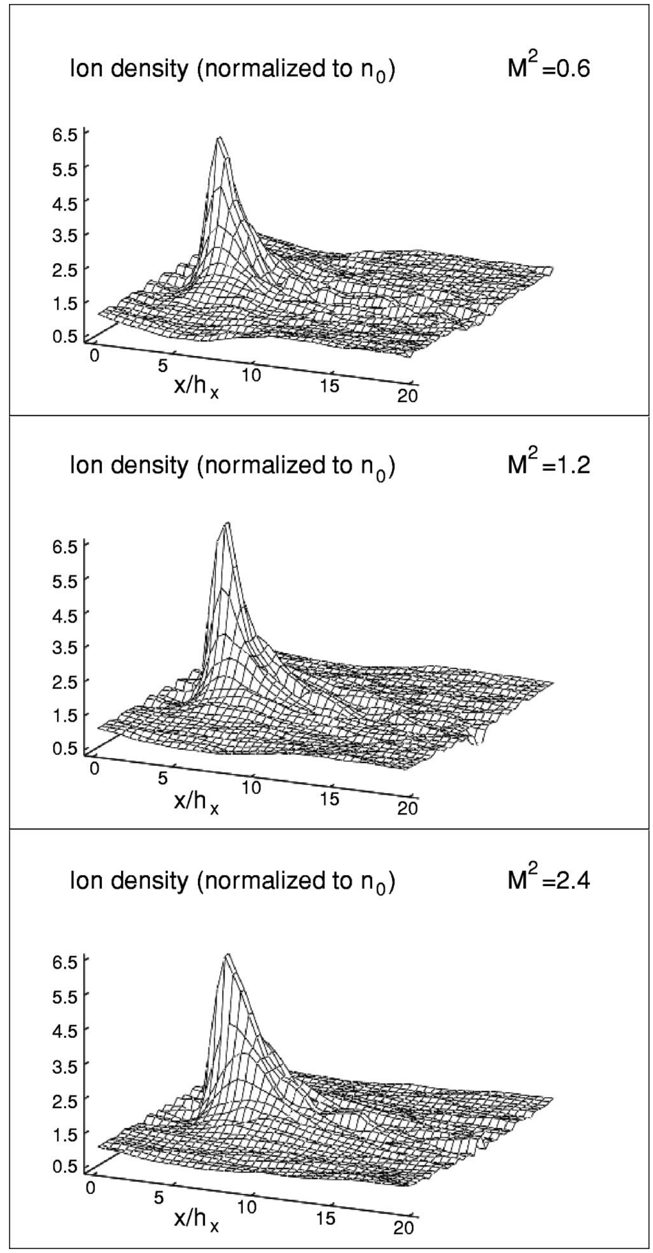

FIG. 2. Surface plot of the ion density for three different velocities of ion flow. The ion focus is mostly formed within the electron Debye length behind the grain.

length $r_{De}=5.256\ \mu$m, ion Debye length $r_{Di}=0.831\ \mu$m, and the Landau length for scattering of the ions on the dust particle by the angle $\pi/2$ is $r_L \equiv Z_d e^2/m_i V_0^2$; for our parameters $r_L=0.6/M^2\ \mu$m.

We note that the direct particle-particle interaction constitutes the most appropriate method for the numerical integration of the equations of motion in studies of basic plasma kinetics. The particle-particle integration method is flexible enough but at a high computational cost. In an implementation of this technique, an algorithm taking advantage of the specific properties of classical Coulomb plasmas was elaborated to significantly decrease the number of arithmetic operations. Central to the method is the determination of the particles nearest to every particle and inclusion of their interaction by using a computational scheme of high-order accuracy (Runge-Kutta of fourth order with an automatically chosen time step). The code realizing the outlined algorithm is written in FORTRAN-90, and it can also be used for studies of various physical objects by varying the particle characteristics as well as the initial and boundary conditions. In particular, simulations using the code have been done for a hydrogen plasma, a plasma with multiply charged ions, an ion plasma, a solid-state plasma, and a system of gravitating masses. The code is supplied with extensive diagnostics of plasma properties based on the tracing of the paths of individual particles. It also includes the calculation of thermodynamic characteristics, kinetic coefficients, micro-field distribution and correlation functions, and the plasma particle distribution functions.

Simulating the charging process, we effectively take into account the real electron/ion mass ratio (we note that in the computational model the electron mass is assumed to be $100m_e$, see Table I) by renormalizing the absorbed charge in the process of the electron-dust charging collision, so that the charge appearing on the grain corresponds to its value for the real electron/ion mass ratio. In the simulation, the ion number density was calculated by averaging within the spherical layer around the macro-particle. The results in the absence of the ion flow demonstrate good agreement with the analytical result for the ion-macroparticle correlation function [23].

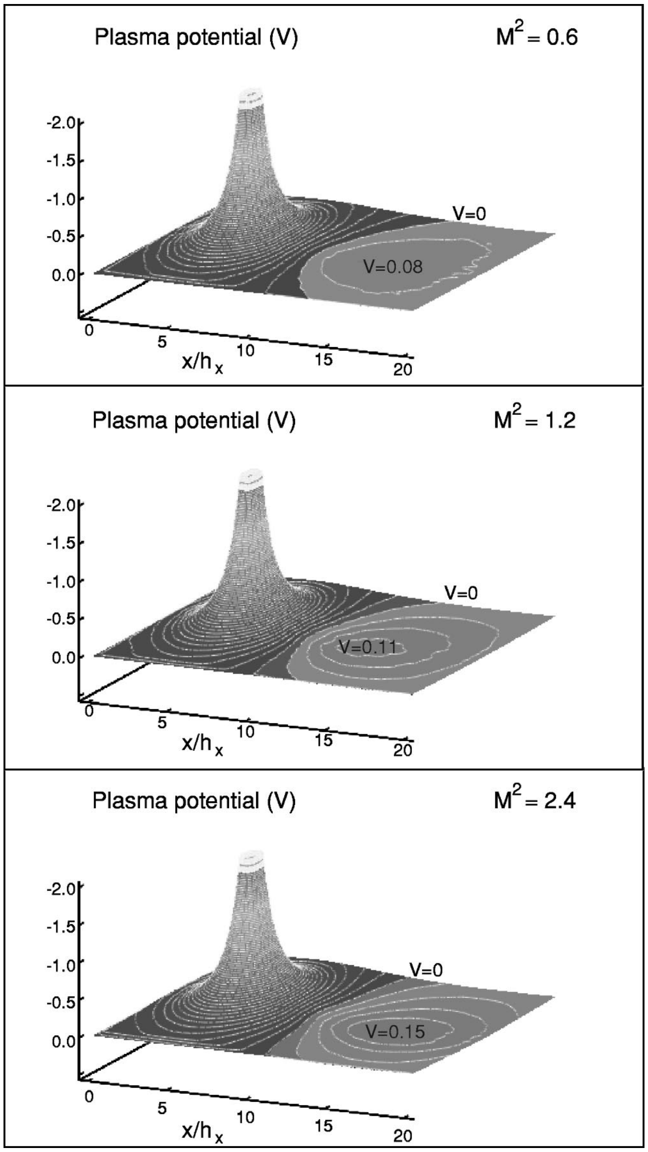

FIG. 3. Surface plot of plasma potential for three different velocities of the ion flow. The plot is presented in the gray scale topograph style. Note that the positive potential well (see the closed contours) is formed behind the dust grain; the lines corresponding to $V=0$ are marked. As the Mach number increases, the well deepens and increases, compare the corresponding regions for $M^2=0.6$, $M^2=1.2$, and $M^2=2.4$; the maximum positive values of the normalized potential in the well are given.

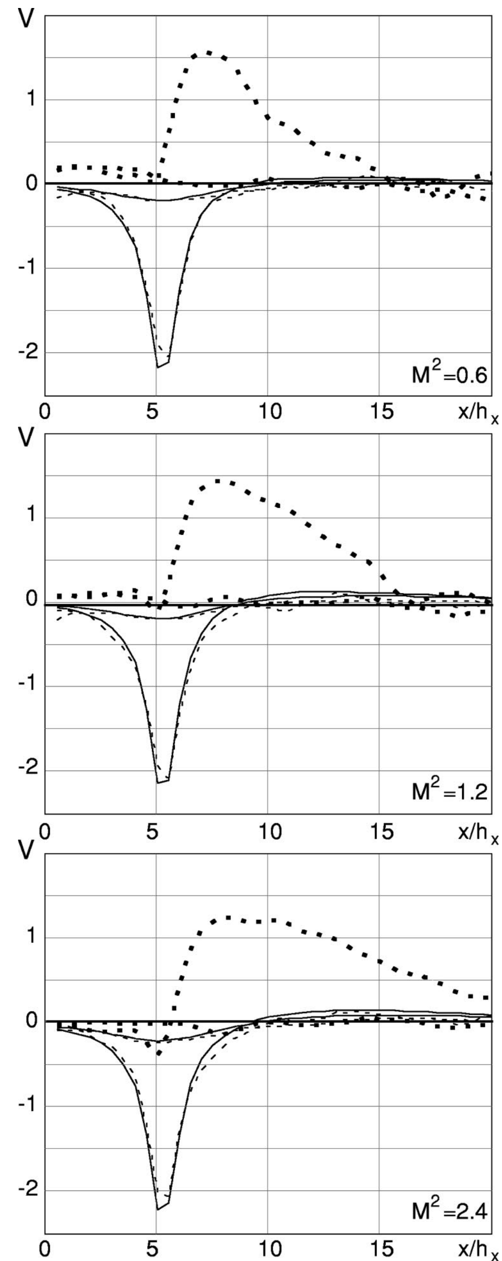

FIG. 4. The distribution of the logarithm of the ion and electron densities and the plasma potential along the lines $y=h_y$ and $y=5h_y$, for three different velocities of ion flow. The solid curves correspond to the electrostatic plasma potential, the dashed curves to the (normalized to 1 V) logarithm of the electron density, and the dotted curves to the similarly normalized logarithm of the ion density. The solid line $V=0$ is also presented.

The total simulation time of the computed physical processes is 3.36×10^{-9} s which is approximately equal to half of the oscillation period of plasma ions oscillating with the ion plasma frequency $\tau_{pi}=6.76\times10^{-9}$ s. The charge of the dust particle was found to fluctuate around $Z_d\approx1000-1100$ weakly depending on the ion flow velocity.

In Fig. 1 we present contour plots of the ion density n_i normalized to $n_0=N_i/L_xL_yL_z$, for three values of the speed of the ion flow (one is subsonic with $M^2=0.6$, and two supersonic, with $M^2=1.2$ and $M^2=2.4$). For better visualization, parts of the simulation volume where $n_i/n_0<1$ and $n_i/n_0>1$, respectively, are presented in the (gray scale) topograph style. A strong ion focus is formed at the distance of a fraction of the electron Debye length behind the dust grain. Figure 2 gives the surface plot of the ion density, with $n_i/n_0\sim6.5$ at the maximum. We see that the maximum value of the density at the ion focus is almost independent of the flow velocity, whereas the characteristic distance of the ion focus from the dust grain increases with increasing flow velocity, being approximately equal to $0.5r_{De}$ for $M^2=2.4$. This characteristic spacing corresponds to an ion focus effect in the near zone of the dust grain, which is a purely kinetic effect [9] not associated with the collective wake field formation. We note that the oscillating wake field which is formed in the wave zone behind the grain [10] cannot form for the considered simulation time (half of the period of the ion oscillations). Another kinetic effect seen from Figs. 1 and 2 is the appearance of precursors in front of the dust grain, which can be attributed to those ions reflected backwards within the radius (around the x axis) of order of the Landau length.

Figure 3 presents a surface plot of the plasma electrostatic potential (in Volts) in a box which is two times shorter in the x direction, i.e., for $0 < x < L_x/2$. The parts where the potential becomes positive, thus forming an attractive region for negatively charged particles, can be seen behind the grain (closed contours at distances $10h_x - 20h_x$). The potential well behind the dust grain deepens, and the characteristic distance of the potential minimum increases with the increase of the flow velocity, approaching r_{De} for $M^2 = 2.4$.

Figure 4 demonstrates the calculated potential distribution (the solid curves) along the lines $y = h_y$ (a deep well around the particle) and $y = 5h_y$ (a shallow well). The dashed curves almost coinciding with the potential distributions correspond to the (normalized to 1 V) logarithm of the electron distribution. We clearly see that the electrons follow with good accuracy the Boltzmann formula $n_e = n_{0e} \exp(-e\phi/T_e)$. The upper dotted curves correspond to the logarithms of the ion density distribution (normalized in the same way) taken along the same lines (the line closest to the dust grain has the largest ion density in the ion focusing region).

To conclude, we have self-consistently demonstrated from first principles by MD calculations that the plasma kinetics around a charged macroscopic body (dust grain) in the presence of an ion flow indeed involves a strong ion focusing behind the grain. We have also confirmed that the most important for the processes involved is the ion time scale; the kinetics of the electrons follows a Boltzmann distribution with good agreement. We note that the time constraints involved (the run time is of the order of the period of ion oscillations at the ion plasma frequency) does not allow us to see the formation of the wake associated with the collective standing ion-acoustic wave (in the case of supersonic flow velocities) within the Mach cone. However, our conclusion is that the electron kinetics are not so important for the ion focusing, and even longer timescale processes such as wake formation, and therefore, to save computer time, future MD simulations can assume that the ions and the dust are immersed in an electron background which obeys a Boltzmann distribution. Another interesting feature observed in our present simulations is the formation of an ion precursor in front of the (stationary) grain; this appears to be a kinetic effect which hardly can occur in a fluid description. However, more studies are necessary to better understand this phenomenon.

This work was supported by the Australian Research Council.

[1] J. H. Chu and Lin I, Phys. Rev. Lett. **72**, 4009 (1994).
[2] H. Thomas, G. E. Morfill, V. Demmel, J. Goree, B. Feuerbacher, and D. Möhlmann, Phys. Rev. Lett. **73**, 652 (1994).
[3] Y. Hayashi and K. Tachibana, Jpn. J. Appl. Phys., Part 2 **33**, L804 (1994).
[4] A. Melzer, T. Trottenberg, and A. Piel, Phys. Lett. A **191**, 301 (1994).
[5] G. Praburam and J. Goree, Phys. Plasmas **3**, 1212 (1996).
[6] D. Samsonov and J. Goree, Phys. Rev. E **59**, 1047 (1999).
[7] J. Goree, G. E. Morfill, V. N. Tsytovich, and S. V. Vladimirov, Phys. Rev. E **59**, 7055 (1999).
[8] G. E. Morfill, H. M. Thomas, U. Konopka, H. Rothermel, M. Zuzic, A. Ivlev, and J. Goree, Phys. Rev. Lett. **83**, 1598 (1999).
[9] V. N. Tsytovich, S. V. Vladimirov, and S. Benkadda, Phys. Plasmas **6**, 2972 (1999).
[10] S. V. Vladimirov and M. Nambu, Phys. Rev. E **52**, 2172 (1995).
[11] F. Melandso and J. Goree, Phys. Rev. E **52**, 5312 (1995).
[12] S. V. Vladimirov and O. Ishihara, Phys. Plasmas **3**, 444 (1996).
[13] V. A. Schweigert, I. V. Schweigert, A. Melzer, A. Homann, and A. Piel, Phys. Rev. E **54**, 4155 (1996).
[14] O. Ishihara and S. V. Vladimirov, Phys. Plasmas **4**, 69 (1997); Phys. Rev. E **57**, 3392 (1998).
[15] S. Benkadda, V. N. Tsytovich, and S. V. Vladimirov, Phys. Rev. E **60**, 4708 (1999).
[16] S. V. Vladimirov and O. Ishihara, Phys. Scr. **60**, 370 (1999).
[17] T. J. Sommerer, M. S. Barnes, J. H. Keller, M. J. McCaughey, and M. J. Kushner, Appl. Phys. Lett. **59**, 638 (1991).
[18] J. P. Boeuf, P. Belenguer, and T. Hbid, Plasma Sources Sci. Technol. **3**, 407 (1994).
[19] D. B. Graves, J. E. Daugherty, M. D. Kilgore, and R. K. Porteous, Plasma Sources Sci. Technol. **3**, 433 (1994).
[20] D. Winske, W. Daughton, D. S. Lemmons, and M. S. Murillo, Phys. Plasmas **7**, 2320 (2000).
[21] R. W. Hockney and J. W. Eastwood, *Computer Simulation Using Particles* (McGraw-Hill, New York, 1981).
[22] S. A. Maiorov, A. N. Tkachev, and S. I. Yakovlenko, Phys. Scr. **51**, 498 (1995).
[23] S. A. Maiorov, Plasma Phys. Rep. **26**, No. 7 (2000).